agronomy

MDPI

Article

Accumulation of Polyphenolics and Differential Expression of Genes Related to Shikimate Pathway during Fruit Development and Maturation of Chinese Olive (*Canarium album*)

Jingrong Cai [1,2], Naiyu Wang [1,2], Junyue Zhao [1,2], Yan Zhao [1,2], Rong Xu [1,2], Fanghao Fu [1,2], Tengfei Pan [1,2], Yuan Yu [1,2,3], Zhixiong Guo [1,2,*] and Wenqin She [1,2,*]

[1] College of Horticulture, Fujian Agriculture and Forestry University, Fuzhou 350002, China
[2] Institute of Storage, Transportation and Preservation of Horticultural Products, Fujian Agriculture and Forestry University, Fuzhou 350002, China
[3] FAFU-UCR Joint Center for Horticultural Biology and Metabolomics, Haixia Institute of Science and Technology, Fujian Agriculture and Forestry University, Fuzhou 350002, China
* Correspondence: gzhhs@fafu.edu.cn (Z.G.); wenqinshe@fafu.edu.cn (W.S.)

Abstract: Phenolics in the Chinese olive (*Canarium album* (Lour.) Raeusch) fruit significantly affect its flavor and quality. The shikimate pathway is a bridge connecting primary metabolism and secondary metabolism through which fixed carbon can be transformed into phenolics. In this study, we aimed to reveal the relationship between the shikimate pathway and phenolic compound biosynthesis. Three Chinese olive fruits (cv. Tanxiang (TX), Changying (CY) and Lingfeng (LF)) with distinct flavor were utilized as materials. The results of this study showed that the synthesis and accumulation of quinate and gallate were active in the Chinese olive fruit. The accumulation amount of phenolic compounds was significantly different among the three cultivars. TX contained the highest content of ellagate, (iso)corilagin, conjugated quercetin and conjugated kaempferol; CY contained the highest content of conjugated luteolin; and LF contained the lowest content of ellagate, conjugated gallate, hyperin, conjugated quercetin, conjugated kaempferol and conjugated luteolin during fruit development. The expression of 3-*dehydroquinate/shikimate dehydrogenase gene-4* (*DHD/SDH-4*), *3-dehydroquinate synthase gene* (*DHQS*), *chorismate synthase gene* (*CS*) and *Chorismate mutase gene-1* (*CM-1*) and shikimate content increased with the maturing of fruit. The gene *3-Deoxy-D-arabino-heptulosonate-7-phosphate synthase gene-1* (*DAHPS-1*) was most expressed in TX, while barely expressed in LF during fruit development. The expression of *CM-1* was highest in CY. *Chorismate mutase gene-2* (*CM-2*) expression was higher in TX and CY during late fruit development. The cultivars with higher expression of *DAHPS-1* and *Chorismate mutase genes* (*CMs*) accumulated more phenolic compounds in fruit. *DAHPS-1* and *CMs* are proposed as key genes for polyphenolic synthesis in the Chinese olive fruit. These results proved that shikimate metabolism had a positive effect on the phenols' synthesis. Our study provides new insight into the regulatory mechanism of the biosynthesis and accumulation of phenolic compounds in the fruit of Chinese olive.

Keywords: *Canarium album*; shikimate pathway; phenolic compounds; flavor; gene expression

check for updates

Citation: Cai, J.; Wang, N.; Zhao, J.; Zhao, Y.; Xu, R.; Fu, F.; Pan, T.; Yu, Y.; Guo, Z.; She, W. Accumulation of Polyphenolics and Differential Expression of Genes Related to Shikimate Pathway during Fruit Development and Maturation of Chinese Olive (*Canarium album*). *Agronomy* **2023**, *13*, 895. https://doi.org/10.3390/agronomy13030895

Academic Editors: Frédéric Marsolais and Dilip R. Panthee

Received: 15 January 2023
Revised: 22 February 2023
Accepted: 14 March 2023
Published: 17 March 2023

Copyright: © 2023 by the authors. Licensee MDPI, Basel, Switzerland. This article is an open access article distributed under the terms and conditions of the Creative Commons Attribution (CC BY) license (https://creativecommons.org/licenses/by/4.0/).

1. Introduction

Chinese olive (*Canarium album* (Lour.) Raeusch) is one of the most popular fruits in southern China; it has unique flavor and is rich in phenolic compounds [1], flavonoids [2] and triterpenoids [2,3]. The fresh fruit of Chinese olive is mostly eaten directly but is also processed into beverages, candy, preserves [4], etc., which depend on different fruit flavors and qualities. 'Tanxiang' is a traditional fresh edible cultivar with strong fruit flavor and less fiber and is easy to chew with good aftertaste. 'Changying' has a hard texture and more wood fiber and is mainly used for processing. 'Lingfeng' is one of the fresh

cultivars selected and bred in recent years; it is fiberless and crisp, with sweet taste and no astringency.

The shikimate pathway is a bridge connecting primary metabolism and secondary metabolism in plants [5]. The shikimate pathway can transform more than 20% of fixed carbon into aromatic compounds, which are precursors for the synthesis of phenols, flavonoids, indole hormones, lignin and other secondary metabolites in plants [6]. Secondary metabolites participate in the regulation of plant growth and development, improve plant resistance and are important components of unique quality elements of horticultural products. The shikimate pathway includes seven enzymatic steps to produce chorismate, a precursor for the synthesis of the aromatic amino acids phenylalanine (Phe), tyrosine (Tyr) and tryptophan (Trp) (Figure 1) [7]. The enzyme 3-deoxy-D-arabino-heptulosonate-7-phosphate synthase (DAHPS) is the first key rate-limiting enzyme in the shikimate pathway; DAHPS catalyzes erythrose-4-phosphate (E4P) and phosphoenolpyruvate (PEP) to form 3-deoxy-D-arabino-heptulosonate-7-phosphate (DAHP). The 3-Dehydroquinate synthase (DHQS) converts DAHP to 3-dehydroquinate (3-DHQ). As a rare bifunctional enzyme in plants, 3-dehydroquinate/shikimate dehydrogenase (DHD/SDH) has an important role in the shikimate pathway, [8]. "Classical" DHD/SDH catalyzes two successive reactions, the dehydration of 3-DHQ to 3-dehy-droshikimate (3-DHS) (reaction 1, DHD activity) and the reversible reduction of 3-DHS to shikimate (reaction 2, SDH activity) [9]. In addition, 3-DHQ can generate quinate catalyzed by quinate dehydrogenase (QDH), and SDH catalyzes the formation of gallate from 3-DHS [10]. Chorismate synthase (CS) is the export enzyme of the shikimate pathway, which catalyzes the final reaction of the shikimate pathway to form chorismite [11]. Chorismate undergoes a claisen rearrangement reaction catalyzed by chorismate mutase (CM) to generate prephenate, a precursor of phenylalanine and tyrosine [12].

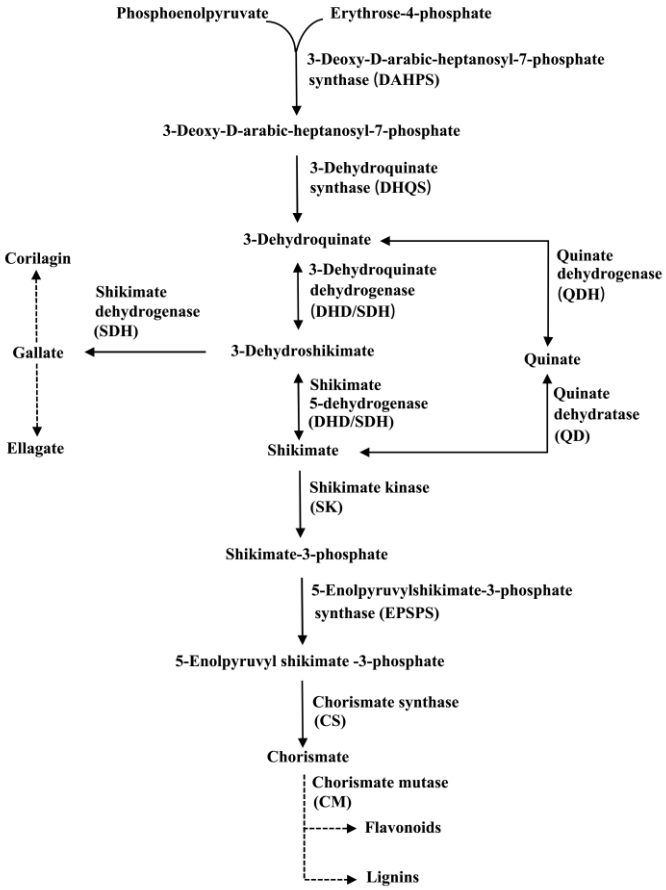


Figure 1. Shikimate pathway and aromatic acid synthesis in plants.

DAHPS plays an important role in the flux regulation of the shikimate pathway, but the regulation mechanism of DAHPS in plants is still unclear. Generally, the plant genome contains two or three *DAHPS* gene members, and they have been isolated from several plants to date [6,13]. Different *DAHPS* genes show tissue specificity and play different roles in regulatory mechanisms [14,15]. There is an *SDH* gene family with 4~6 family members in *Vitis vinifera* L. [16], *Camellia sinensis* (L.) [17] and other plants. Some members of this family are used to code DHD/SDH, and the others are used to code QDH [10]. These family members all have more than 50% sequence identity at the amino acid level, but there are slight differences in the residue composition and geometric structure of the activation site among the different isoenzymes [18,19]. There are at least two kinds of CM isozymes in plants, which have some differences in biological characteristics, the activity regulation mechanism and cellular localization [20]. *Arabidopsis thaliana* (L.) Heynh. chorismate mutase 1 (AtCM1) participates in the synthesis of phenylalanine through the arogenate pathway in plastids, but how the cytoplasm-located *Arabidopsis thaliana* chorismate mutase 2 (AtCM2) is involved in the phenylalanine pathway in the cytoplasm is unknown [21]. The cytoplasmic *Petunia hybrida* Vilm. chorismate mutase 2 (PhCM2) participates in the biosynthesis of phenylalanine through a phenylpyruvate pathway similar to that of microorganisms [21]. The shikimate pathway is related to the secondary metabolism at the gene expression or enzyme activity level [22–24]. Inhibition of *DAHPS* or *DHD/SDH* expression has been demonstrated to lead to severe growth retardation and reduction in some secondary metabolites such as lignin and chlorogenate in potato and tobacco [25,26].

The shikimate pathway is the starting point and necessary pathway of phenolic synthesis [27]. Plants and microorganisms use the shikimate pathway to regulate the carbon flux entering the secondary metabolite synthesis pathway. If the carbon flux in and out of the shikimate pathway is inhibited or promoted, the biosynthesis of phenolic substances connected to its downstream section will be affected. *SDH* family members related to gallic acid synthesis were highly expressed in plants with high amounts of hydrolysable tannins (HTS), such as strawberry and eucalyptus, or galloylated flavan-3-ols, such as in tea plants, grape and persimmon [8]. However, species without these members, such as Arabidopsis, tobacco, tomato and orange, do not produce HTs and galloylated tannins [16]. The balance of structural gene expression in shikimate and flavonoid biosynthesis leads to a difference in proanthocyandin accumulation between pollination-constant and non-astringent type (PCNA) and normal (non-PCNA)-type fruits of persimmon (*Diospyros kaki* Thunb.) [28].

In Chinese olive fruits, as the most important components, phenolic substances are the focus of many reports. In an earlier study, we found that phenolic substances in Chinese olive fruits were closely related to their flavor and quality [29]. Meanwhile, lignin played an important role in the fruit texture and quality of Chinese olive [30]. Fruits of the cultivars with high contents of phenolic substance had a rich flavor, fruits of the cultivars with low contents of phenolic substance were less astringent and fruits of the cultivars with high contents of lignin were hard and difficult to chew. The shikimate pathway might be involved in the differential biosynthesis and accumulation of polyphenolics in the fruit of different cultivars. Most studies on the phenolic metabolism regulatory mechanism in Chinese olive have focused on the downstream section of the shikimate pathway, such as phenylpropanoid and flavonoid pathways; however, to date, little is known about the involvements of the shikimate metabolism of the fruit.

In this study, Chinese olive fruits 'Tanxiang' (TX), 'Changying' (CY) and 'Lingfeng' (LF) were selected as experiment materials. Shikimate, quinate and phenolic compounds' contents in the fruits at different developmental stages were measured by Ultra-Performance Liquid Chromatography Tandem Mass Spectrometry (UPLC-MS); the expression of the genes related to the shikimate metabolism including *DAHPSs*, *DHQS*, *DHD/SDHs*, *CS* and *CMs* were analyzed using real-time quantitative PCR (RT-qPCR). This work provides new insight into further elucidating the regulatory mechanism of the biosynthesis and accumulation of polyphenolics in the Chinese olive fruit.

2. Materials and Methods

2.1. Plant Material

'Changying' (CY), 'Tanxiang' (TX) and 'Lingfeng' (LF) were selected as the experiment materials. Three 10-year-old trees with the same growth trends were selected for each cultivar. CY and TX were located in the Sweet Chinese Olive Base of Chinese Olive Specialty Cooperative in Shiyinshan, Minqing County, Fuzhou, Fujian Province (118°86′ east longitude, 26°29′ north latitude), and LF was located in the Juiyuan Chinese Olive Specialty Cooperative in Minqing County, Fuzhou, Fujian Province (118°51′ east longitude, 26°14′ north latitude). The fruits were picked for the first time on the 50th day after flowering (DAF), and then were picked every 20 days until the 170th DAF. Twenty fruits were selected randomly from each tree. A total of 60 fruits from each cultivar at each stage were randomly assigned into three groups with 20 fruits per group serving as biological replicates. The fruit pits were removed, and the fruit flesh was cut into slices, mixed, weighed, then frozen in liquid nitrogen and stored at −80 °C.

2.2. Methods

2.2.1. Extraction of Shikimate, Quinate and Phenolic Compounds

Each cultivar was provided with three biological replicates in each stage, and a total of 63 samples were taken from the refrigerator at −80 °C for the extraction of compounds. Polyphenolics, containing shikimate and quinate, were extracted according to the method as described by Reichel et al. [31] with a slight modification. Fruit flesh (2 g) was grounded then extracted with methanol (20 mL) for 30 min under continuous vibrating. After centrifugation at 12,000 rpm for 15 min in an Allegra 64R (Beckman Coulter, Brea, CA, USA), the supernatant was decanted, then the pellet was suspended in methanol (10 mL) before further centrifugation (15 min, 12,000 rpm). Solid residue was extracted with 20 mL of acetone/water (7:3, *v/v*) for 24 h, centrifuged (15 min, 12,000 rpm), and then the supernatant was decanted and the solid residue was extracted with 20 mL of acetone/water (7:3, *v/v*) for 30 min under continuous vibrating before further centrifugation (15 min, 12,000 rpm). The pellet was suspended in 20 mL of acetone/water (7:3, *v/v*) before the last centrifugation (15 min, 12,000 rpm). Trifluoroacetic acid concentrations of 0.01 and 0.1% (*v/v*) were added to the above methanol and aqueous acetone before extraction to prevent oxidation of phenolic compounds, respectively. The methanolic supernatants of the first two centrifugation steps were combined in a glass separation funnel with purified water (5 mL) and extracted three times using 1 × 20 mL and 2 × 10 mL of petroleum ether (boiling range of 40~60 °C). Methanol phase and acetone phase were evaporated in vacuo at 35 °C, respectively. Dried residue was dissolved with 5 mL methanol/water (7:3, *v/v*, containing 0.1% formic acid) to obtain total phenol extract.

The conjugated phenolic forms in the total extract were obtained by acid hydrolysis as described by Muir et al. [32] with a slight modification. Total phenolic extract (2 mL) was hydrolyzed in 2 mL methanol/water (9:1, *v/v*) and 1 mL 6 M HCl for 60 min at 90 °C. The hydrolyzed extracts were cooled on ice, diluted with 10 mL of methanol/water (8:2, *v/v*) and evaporated in vacuo at 35 °C. The dried residue was dissolved in 2 mL methanol (containing 0.1% formic acid).

All the extracts were filtered through 0.22 μm nylon 66 filters before UPLC-MS analysis.

2.2.2. UPLC-MS Analysis

UPLC was carried out on an ACQUITY UPLC I-Class PLUS system (Waters, Milford, MA, USA) using an ACQUITY UPLC® BEH- C18 column (1.7 μm, 2.1 × 100 mm, Waters, Milford, MA, USA). An ACQUITY UPLC® tunable UV detector (Waters, Milford, MA, USA) was used to record online spectra (254 nm and 280 nm). Gradient elution was performed with 0.1% (*v/v*) formic acid/water (solvent A) and methanol (containing 0.1% formic acid, solvent B) at a constant flow rate of 0.25 mL/min. The linear gradient profile was as follows: 90% A and 10% B at the start, then to 20% A and 80% B at 10 min, remaining at 10% A and

90% B from 12 to 15 min, and falling back to 90% A and 10% B at 16.5 min, remaining at 90% A and 10% B to 20 min at the end.

ESI-MS analyses were performed with an ACQUITY UPLC-QDa (Waters, Milford, MA, USA) mass spectrometer. Mass spectra was achieved by electrospray ionization in negative modes. The following ion optics were used: capillary 0.8 kV and cone 15 V. Continuous mass spectra were obtained by scanning from 100 to 1200 *m/z*. MRM quantitative parameters of shikimate, quinate and phenolic compounds' mass spectrometry are shown in Appendix A (Table A1).

The peak area coefficient of external standard was used to calculate the content of individual component in the fruit, and the content was expressed in $mg \cdot g^{-1} \cdot FW$.

2.2.3. Gene Expression Analyses

The processed sample was taken from the refrigerator at −80 °C for the extraction of total RNA. Total RNA was extracted from fruit flesh samples of three Chinese olive cultivars at seven development stages using pBIOZOL Plant total RNA extraction reagent (BSC55, Bioer, Hangzhou, China). Total RNA was verified by demonstrating the existence of intact ribosomal bands on 1% agarose gel and the absorbance ratios (A260/280) of 1.8 to 2.0 on a BioSpectrometer basic nucleic acid protein tester (Eppendorf, Hamburg, Germany). Purified RNA was reverse transcribed with a PrimeScript™ RT reagent Kit with gDNA Eraser (Perfect Real Time) for RT-qPCR (Takara, Dalian, China). RT-qPCR was carried out with gene-specific primers using 2 × RealStar Fast SYBR qPCR Mix (GenStar, Beijing, China). Primers (Appendix A (Table A2)) for RT-qPCR were designed according to shikimate-metabolism-related gene sequences in Chinese olives (*DAHPS-1*, *DAHPS-2*, *DAHPS-3*, *DHQS*, *DHD/SDH-1*, *DHD/SDH-2*, *DHD/SDH-3*, *DHD/SDH-4*, *DHD/SDH-5*, *CS*, *CM-1* and *CM-2*). The above genes were cloned by our research team and their open reading frame (ORF) sequences were shown in Supplementary Materials (Table S1). *Actin7* was used as a reference gene [33]. RT-qPCR was performed in three replicates for each sample with three independent biological repeats, and relative expression was calculated with $2^{-\Delta\Delta CT}$ method [34].

2.2.4. Data Analysis

Microsoft Excel 2016 (Microsoft, Redmond, WA, USA) was used to analyze the data and make graphs. The analysis of variance (ANOVA) was performed using SPSS 20.0 software (IBM, Armonk, NY, USA). Duncan's multiple range test was used to compare the means. Pearson's correlation analyses were calculated using "Correlation Plot" packages in Origin2021 (OriginLab, Northampton, MA, USA) to determine the correlation between genes and the correlation between genes and components.

3. Results

3.1. Changes in Shikimate, Quinate and Phenolic Substances during Fruit Development

The shikimate content in the development of Chinese olive fruits among the three cultivars remained steady until the 150th DAF, when the amount increased 0.5~3-fold (Figure 2A). The highest value of shikimate content in TX (0.04 $mg \cdot g^{-1}$) and CY (0.03 $mg \cdot g^{-1}$) appeared in both on the 150th DAF (Figure 2A), while LF (0.04 $mg \cdot g^{-1}$) reached the highest value on the 170th DAF (Figure 2A).

The quinate content was very high (18.8~26.80 $mg \cdot g^{-1}$) in Chinese olive fruits compared with shikimate (Figure 2B). The quinate content in TX (24.42 $mg \cdot g^{-1}$), CY (26.80 $mg \cdot g^{-1}$) and LF (23.84 $mg \cdot g^{-1}$) all reached the highest value on the 170th DAF (Figure 2B).

During fruit development, the changes in free ellagate content differed from each other among the three Chinese olive cultivars (Figure 2C). The free ellagate content in TX was the highest (0.26 $mg \cdot g^{-1}$) on the 50th DAF then decreased gradually (Figure 2C). The content of free ellagate in CY increased first and then decreased, reaching the peak value (0.16 $mg \cdot g^{-1}$) on the 170th DAF (Figure 2C). The free ellagate content in LF fluctuated and changed slightly during the whole development, reaching the highest value (0.09 $mg \cdot g^{-1}$)

on the 170th DAF (Figure 2C). During the fruit development, the free ellagate content in TX and CY was higher than that in LF.

In general, the (iso)corilagin content showed a gradual upward trend among the three Chinese olive cultivars (Figure 2D). The (iso)corilagin content of TX was higher than CY and LF from the 130th to 170th DAF and reached the highest value (0.34 mg·g^{-1}) on the 170th DAF (Figure 2D). The highest content (0.26 mg·g^{-1}) of (iso)corilagin in CY appeared on the 150th DAF, while LF reached the highest value (0.30 mg·g^{-1}) on the 170th DAF (Figure 2D).

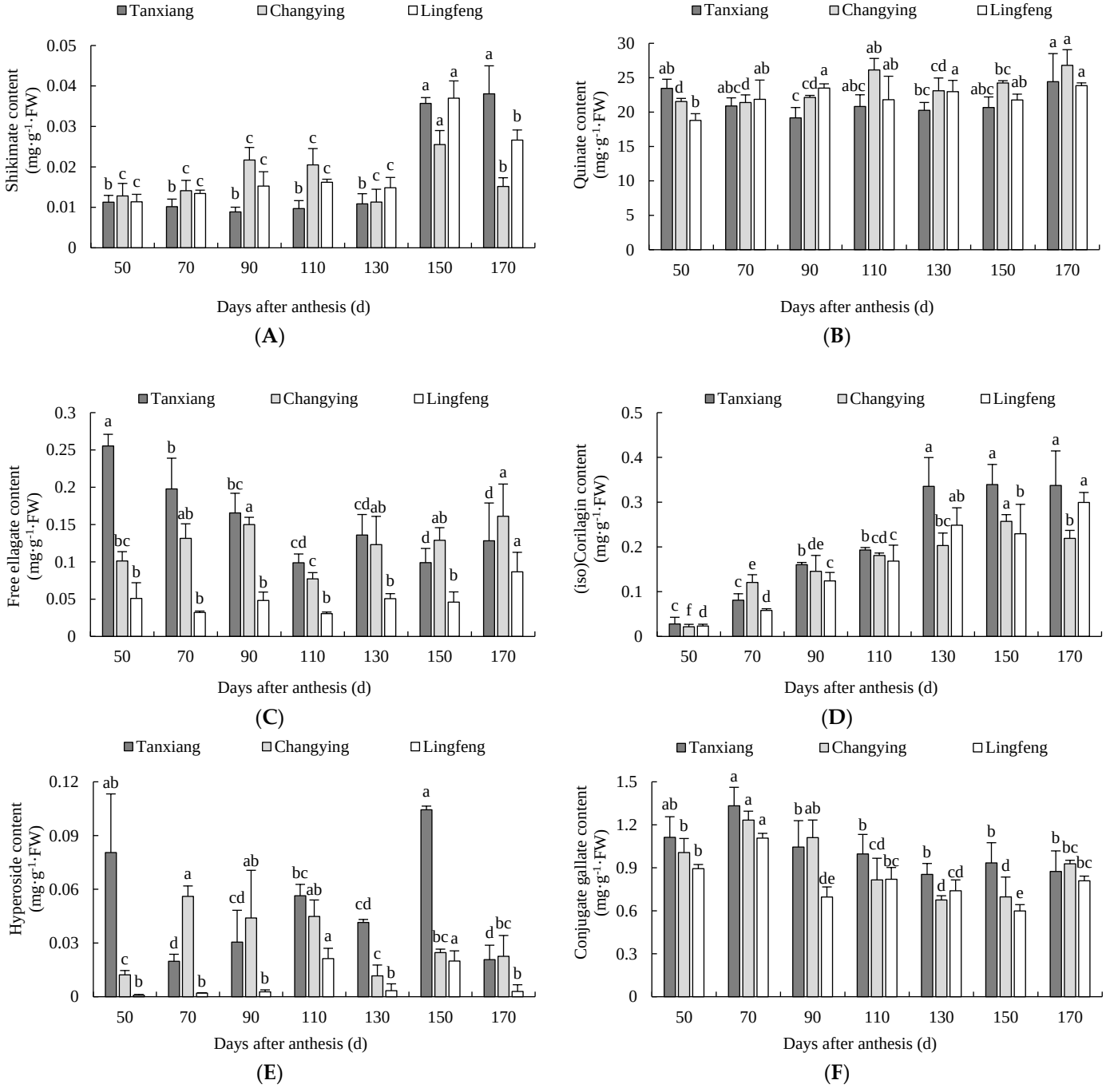


Figure 2. *Cont.*

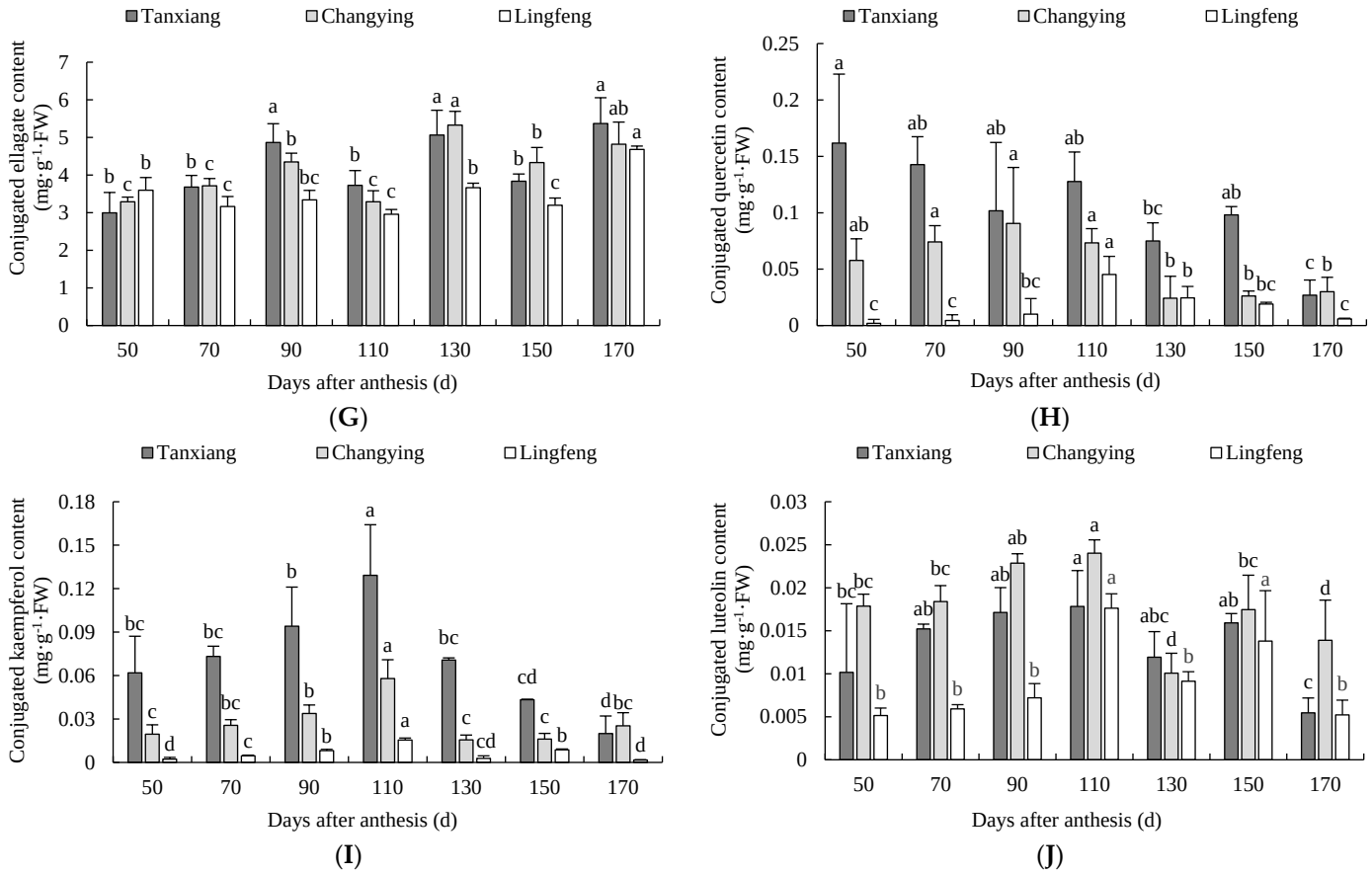


Figure 2. Content of shikimate, quinate and phenolic substances in Chinese olive fruit at different developmental stages. Bars represent the standard deviation for three biological replicates. Different letters indicate significant differences among different stages of the same cultivars ($p < 0.05$). (**A**) Shikimate, (**B**) quinate, (**C**) free ellagate, (**D**) (iso)corilagin, (**E**) hyperoside, (**F**) conjugated gallate, (**G**) conjugated ellagate, (**H**) conjugated kaempferol, (**I**) conjugated quercetin and (**J**) conjugated luteolin.

However, the hyperoside content changed differently among the three Chinese olive cultivars. The hyperoside content in TX was higher on the 50th DAF and 150th DAF, increased first and then decreased from the 70th DAF to 130th DAF, and showed a downward trend on the 170th DAF (Figure 2E). The hyperoside content in CY increased first and then decreased, reaching the highest value (0.06 $mg \cdot g^{-1}$) on the 70th DAF (Figure 2E). The hyperoside content in LF increased on the 110th DAF and 150th DAF, reaching the highest value (0.02 $mg \cdot g^{-1}$) on the 110th DAF (Figure 2E). The hyperoside content in LF was lower than TX and CY during the fruit development (Figure 2E).

The conjugated gallate content was between 0.60 $mg \cdot g^{-1}$ and 1.33 $mg \cdot g^{-1}$ among the three Chinese olive fruits, which was the second highest among the phenolic substances determined (Figure 2F). The content decreased and remained stable in TX after the 70th DAF (Figure 2F). The content gradually decreased on the 90th DAF to the 150th DAF and increased slightly on the 170th DAF in CY and LF (Figure 2F).

The conjugated ellagate content was the highest among the phenolic substances determined in Chinese olive fruits, which was 2.25 to 8.95 times higher than conjugated gallate (Figure 2G). During fruit development, the conjugated ellagate content in TX and CY decreased slightly on the 110th DAF and 150th DAF and showed an increasing trend in other periods (Figure 2G). The highest value of conjugated ellagate in TX (5.37 $mg \cdot g^{-1}$) and CY (5.33 $mg \cdot g^{-1}$) appeared on the 170th DAF and 130th DAF, respectively (Figure 2G). LF showed the same trend as TX and CY except for a small decrease on the 70th DAF,

while the highest value (4.68 mg·g^{-1}) in LF appeared on the 170th DAF (Figure 2G). The differences in conjugated ellagate content among the three Chinese olive cultivars during fruit development were small (Figure 2G).

The conjugated quercetin content in TX decreased gradually during the whole process, and the highest content (0.16 mg·g^{-1}) appeared on the 50th DAF (Figure 2H). The conjugated quercetin content in CY and LF increased first and then decreased. CY (0.09 mg·g^{-1}) and LF (0.05 mg·g^{-1}) reached the highest value on the 90th DAF and 110th DAF, respectively (Figure 2H). From the 50th DAF to 150th DAF, the conjugated quercetin content in TX was the highest among the three Chinese olive cultivars (Figure 2H).

The conjugated kaempferol content rose first and then declined among the three Chinese olive fruits (Figure 2I). The highest values of conjugated kaempferol content in TX (0.13 mg·g^{-1}), CY (0.06 mg·g^{-1}) and LF (0.02 mg·g^{-1}) all appeared on the 110th DAF (Figure 2I). The conjugated kaempferol content in TX was obviously higher than CY and LF except for the 170th DAF, and the content in LF among the three cultivars was the lowest in all periods (Figure 2I).

The conjugated luteolin content continued to increase from the 50th DAF to 110th DAF and fluctuated from the 130th DAF to 170th DAF among the three Chinese olive fruits. The content of conjugated luteolin in CY was always higher than TX and LF except for the 110th DAF (Figure 2J). The highest content (0.02 mg·g^{-1}) of conjugated luteolin in CY appeared on the 110th DAF (Figure 2J). The content of conjugated luteolin in LF was lower than the other two cultivars at all stages, and the content (0.01 mg·g^{-1}) in LF was the highest on the 150th DAF (Figure 2J). The content of conjugated luteolin in TX was between CY and LF and reached the highest value (0.02 mg·g^{-1}) on the 110th DAF (Figure 2J).

3.2. Changes in Shikimate-Metabolism-Related Genes' Expression during Fruit Development

3.2.1. Expression Changes of *DAHPSs*

During fruit development, the *DAHPS-1* expression in TX increased first and then decreased, and that in CY fluctuated (Figure 3A). The expression in the late stage of fruit development was higher than the early stage in CY (Figure 3A). However, *DAHPS-1* expressed at a barely detectable level in LF during all stages (Figure 3A). In addition, the expression level of *DAHPS-1* in TX was higher than CY (Figure 3A).

The *DAHPS-2* expression among the three Chinese olive cultivars showed a fluctuating trend (Figure 3B). The highest expressions of *DAHPS-2* in TX, CY and LF all appeared on the 50th DAF (Figure 3B). The highest expression of LF was 62.50% of TX and 55.16% of CY (Figure 3B). The *DAHPS-2* expression was higher in CY than TX and LF except for the 130th DAF and 150th DAF (Figure 3B).

The *DAHPS-3* expression fluctuated among the three Chinese olive fruits (Figure 3C). The highest expression of *DAHPS-3* in TX appeared on the 170th DAF, which in CY and LF both appeared on the 50th DAF (Figure 3C).

3.2.2. Expression Changes of *DHQS*

The *DHQS* expression increased gradually in TX and CY from the 70th DAF to 170th DAF (Figure 4). The expression in LF decreased gradually from the 50th DAF to 90th DAF, then increased from the 90th DAF to 150th DAF (Figure 4). The *DHQS* expression in TX and CY was the highest on the 170th DAF, which was 20 days later than LF (Figure 4).

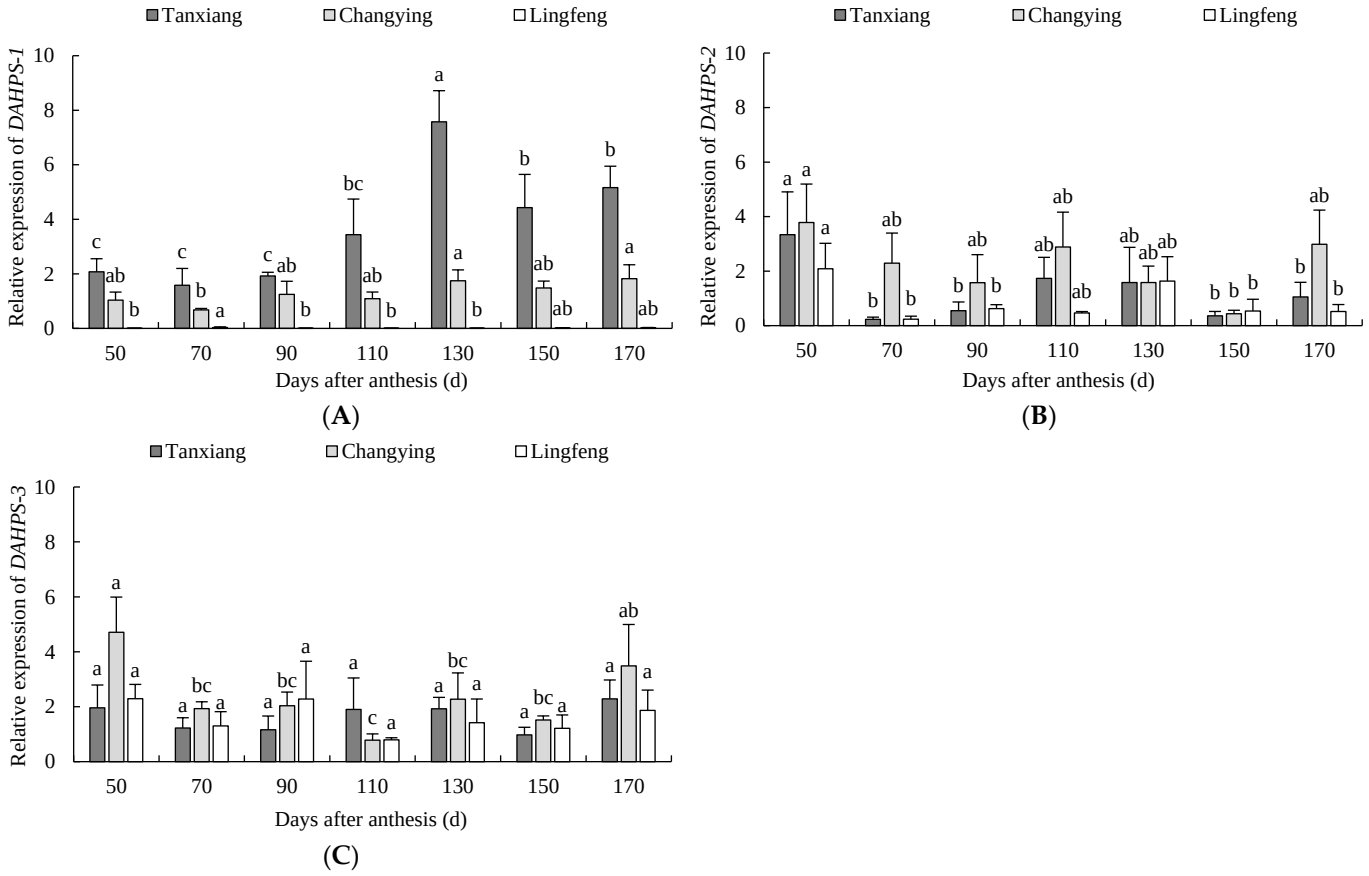


Figure 3. Expression of *DAHPSs* in Chinese olive fruit at different developmental stages. Bars represent the standard deviation for three biological replicates. Different letters indicate significant differences among different stages of the same cultivars ($p < 0.05$). (**A**) *DAHPS-1*, (**B**) *DAHPS-2* and (**C**) *DAHPS-3*.

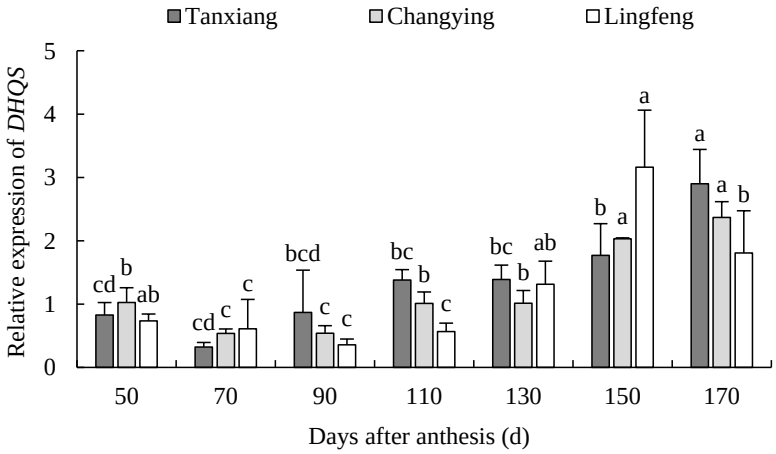


Figure 4. Expression of *DHQS* in Chinese olive fruit at different developmental stages. Bars represent the standard deviation for three biological replicates. Different letters indicate significant differences among different stages of the same cultivars ($p < 0.05$).

3.2.3. Expression Changes of *DHD/SDHs*

DHD/SDH-1 expression rose firstly and then declined in the three Chinese olive cultivars during fruit development (Figure 5A). The *DHD/SDH-1* expressions in TX, CY and LF all reached the highest values on the 110th DAF (Figure 5A). After the 110th DAF, the *DHD/SDH-1* expression levels in the three cultivars showed a decreasing trend, and the expression level from the 130th DAF to 170th DAF in LF was significantly lower than the 110th DAF (Figure 5A).

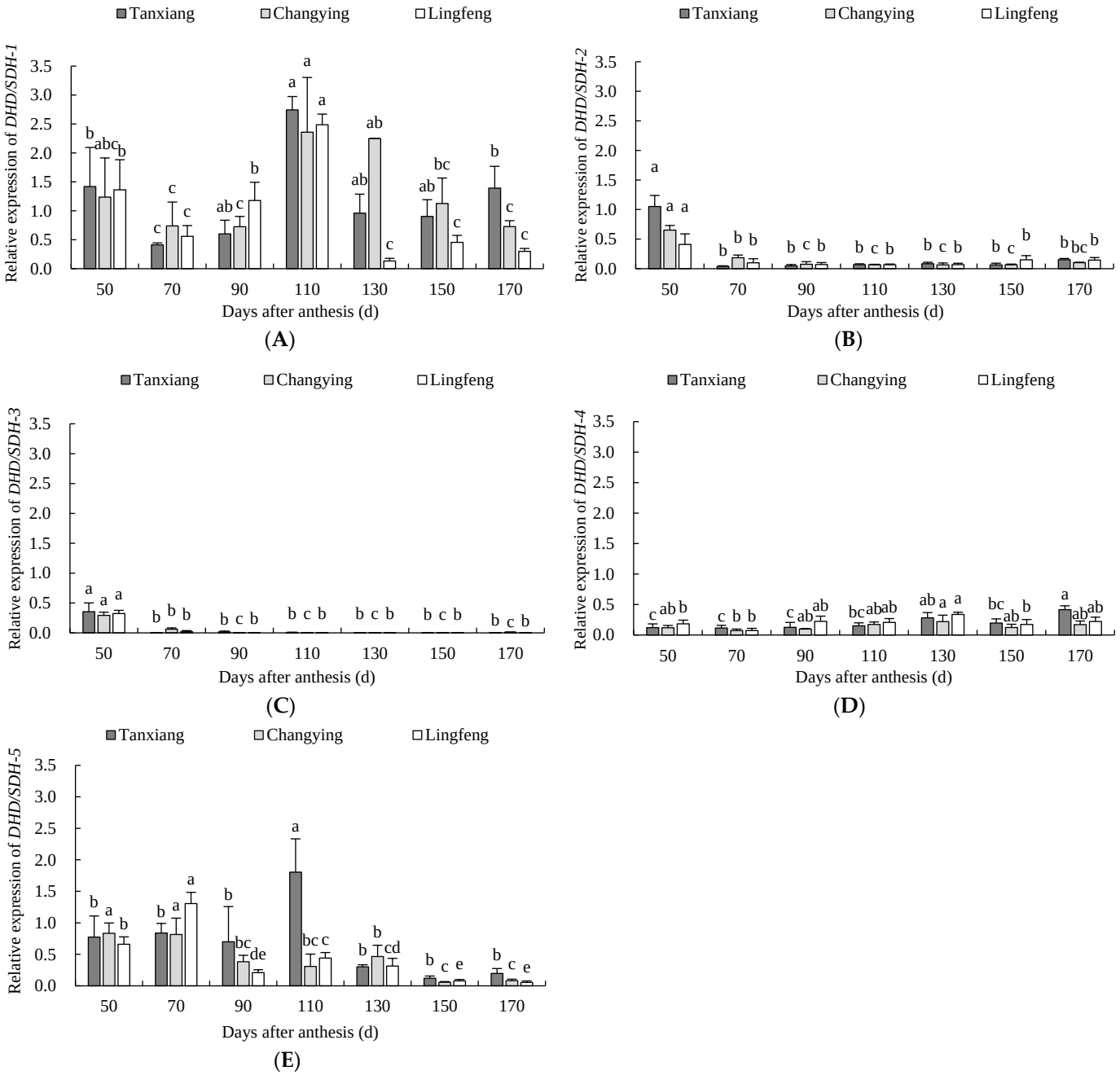


Figure 5. Expression of *DHD/SDHs* in Chinese olive fruit at different developmental stages. Bars represent the standard deviation for three biological replicates. Different letters indicate significant differences among different stages of the same cultivars ($p < 0.05$). (**A**) *DHD/SDH-1*, (**B**) *DHD/SDH-2*, (**C**) *DHD/SDH-3*, (**D**) *DHD/SDH-4* and (**E**) *DHD/SDH-5*.

The three cultivars all reached the highest expression of *DHD/SDH-2* on the 50th DAF, while TX was significantly higher than CY and LF (Figure 5B). The expression among the three cultivars decreased sharply and stayed at a low level after the 70th DAF (Figure 5B).

The trends of *DHD/SDH-3* expression were similar to *DHD/SDH-2* among the three Chinese olive fruits during fruit development (Figure 5C). The *DHD/SDH-3* expressions among the three cultivars were the highest on the 50th DAF and decreased sharply on 70th DAF (Figure 5C).

The *DHD/SDH-4* expression in TX increased gradually during fruit development, and the highest expression in TX appeared on the 170th DAF (Figure 5D). The *DHD/SDH-4* expression in CY and LF showed a fluctuating trend, and that in CY and LF was the highest on the 130th DAF (Figure 5D).

The *DHD/SDH-5* expression rose first and then declined in TX and LF, while that in CY gradually decreased (Figure 5E). The *DHD/SDH-5* expression in TX was the highest on the 110th DAF, which was significantly higher than the other two cultivars (Figure 5E). However, CY and LF reached the highest values on 50th DAF and 70th DAF, respectively (Figure 5E). *DHD/SDH-5* showed a weak expression among the three cultivars from the 150th DAF to 170th DAF (Figure 5E).

The *DHD/SDHs* expression levels were different during fruit development among the three cultivars. *DHD/SDH-1* and *DHD/SDH-5* had relatively high expression levels and expression levels of *DHD/SDH-3* and *DHD/SDH-4* were relatively low (Figure 5).

3.2.4. Expression Changes of *CS*

The *CS* expression rose gradually in TX and CY, which fluctuated in LF (Figure 6). The highest expression of *CS* in TX and CY appeared on the 170th DAF in both, and LF was the highest on the 150th DAF (Figure 6).

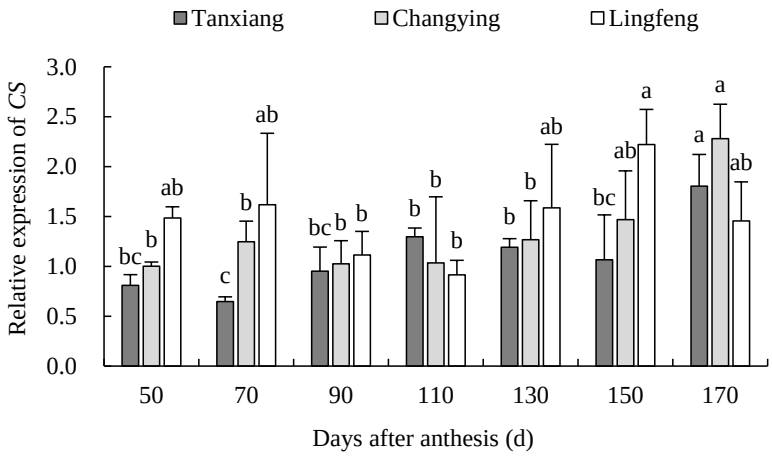


Figure 6. Expression of *CS* in Chinese olive fruit at different developmental stages. Bars represent the standard deviation for three biological replicates. Different letters indicate significant differences among different stages of the same cultivars ($p < 0.05$).

3.2.5. Expression Changes of *CMs*

The *CM-1* expression rose gradually in TX and CY during fruit development (Figure 7A). The expression trend in LF was the same as TX and CY from the 90th DAF to 170th DAF (Figure 7A). The *CM-1* expression in CY was higher than TX and LF, except for the 130th DAF (Figure 7A).

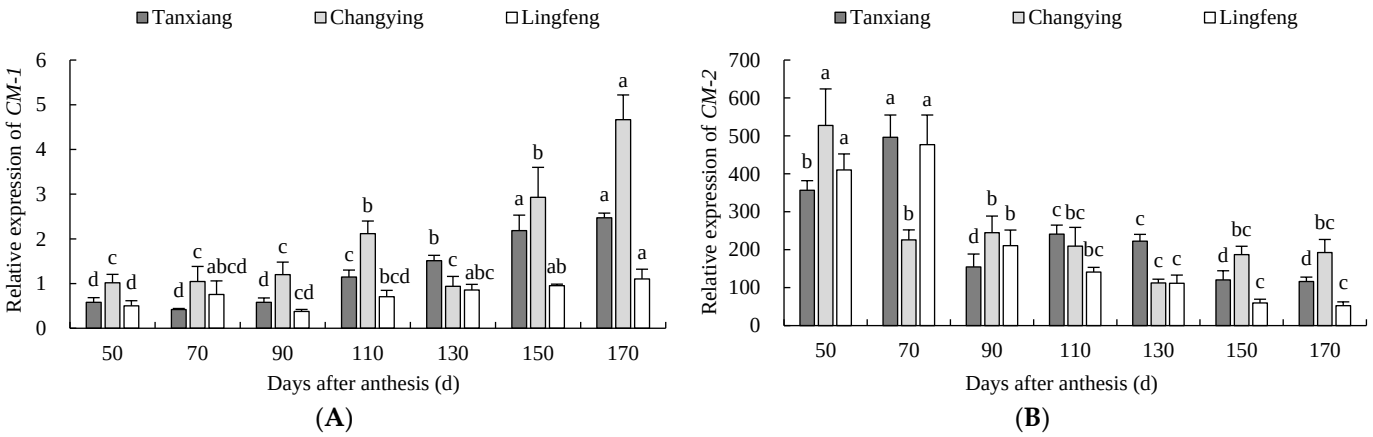


Figure 7. Expression of *CMs* in Chinese olive fruit at different developmental stages. Bars represent the standard deviation for three biological replicates. Different letters indicate significant differences among different stages of the same cultivars ($p < 0.05$). (**A**) *CM-1* and (**B**) *CM-2*.

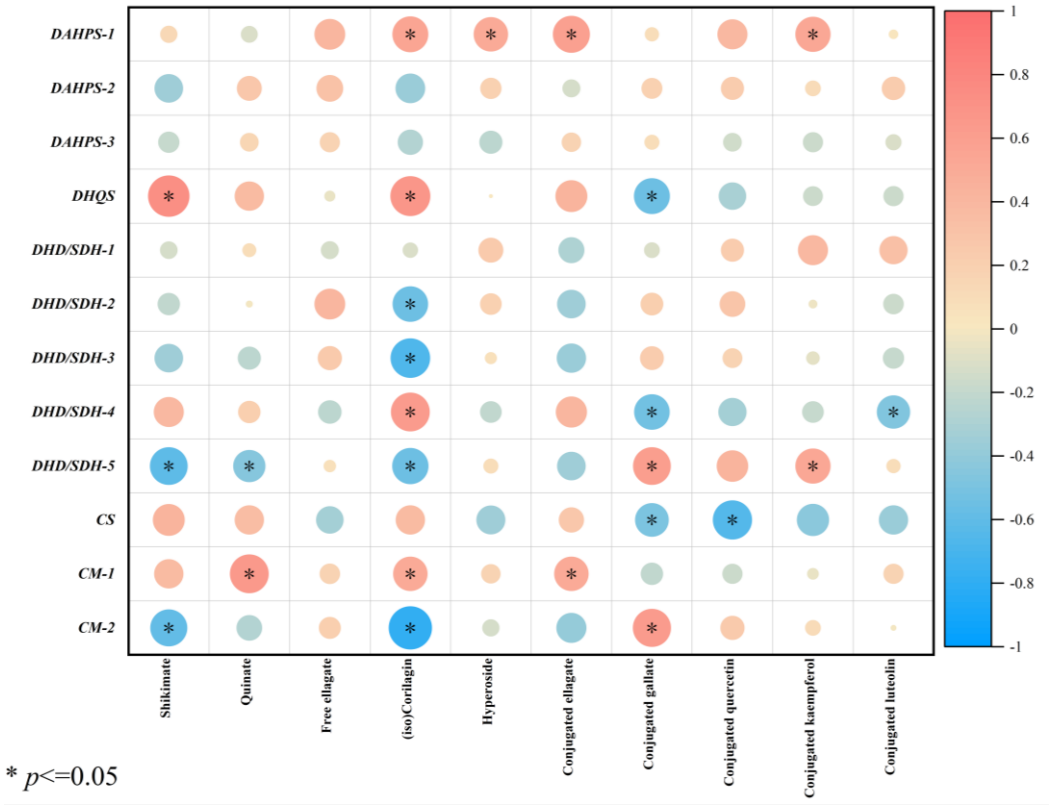
The *CM-2* expression in CY and LF showed a decreasing trend during fruit development, which in TX showed the same trend as LF from the 110th DAF to 170th DAF (Figure 7B). The *CM-2* expression in TX and CY was higher than LF from the 110th DAF to 170th DAF (Figure 7B).

CM-2 expression level was significantly high during fruit development among the three Chinese olive fruits, and *CM-2* expression was 50 to 500 times higher than *CM-1* among the three cultivars (Figure 7).

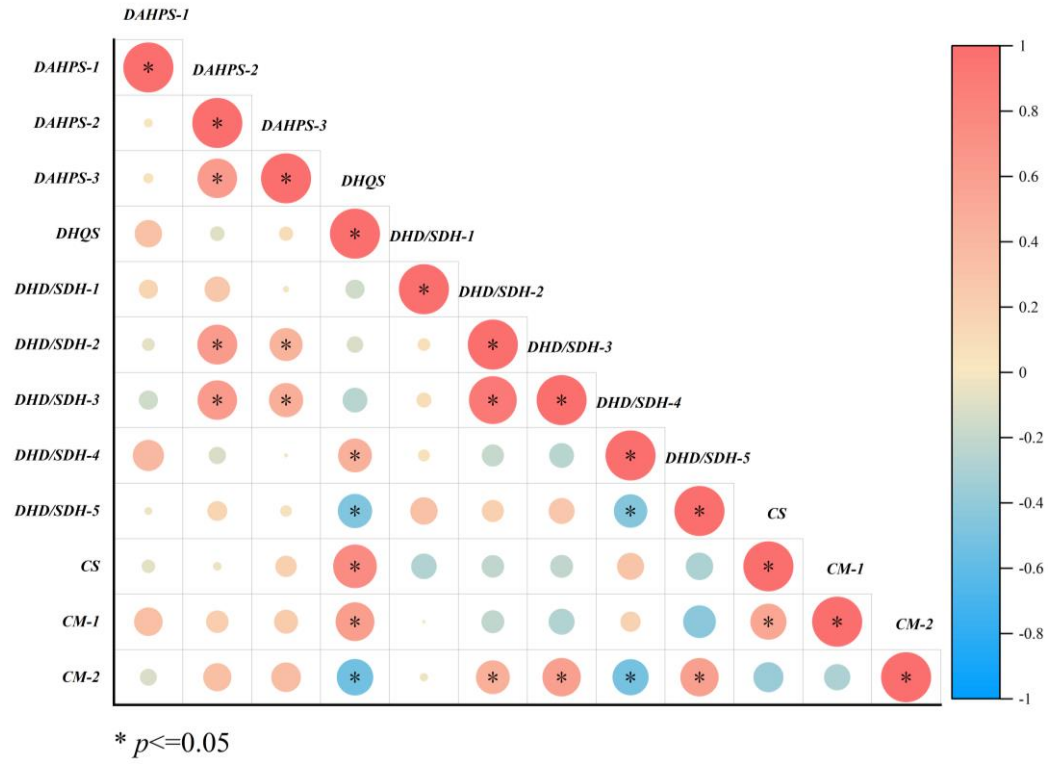
3.3. Correlation Analysis

The correlation analysis between genes and components showed that *DAHPS-1* expression was significantly positively correlated with (iso)corilagin, hyperoside, conjugated ellagate and conjugated kaempferol content (Figure 8A). *DHQS* expression was significantly positively correlated with shikimate and (iso)corilagin content but significantly negatively correlated with conjugated gallate content (Figure 8A). *DHD/SDH-2* and *DHD/SDH-3* expression was significantly negatively correlated with (iso)corilagin content (Figure 8A). *DHD/SDH-4* expression was significantly positively correlated with (iso)corilagin content but significantly negatively correlated with conjugated gallate and conjugated luteolin content (Figure 8A). *DHD/SDH-5* expression was significantly positively correlated with conjugated gallate and conjugated keampferol content but significantly negatively correlated with shikimate, quinate and (iso)corilagin content (Figure 8A). *CS* expression was significantly negatively correlated with conjugated gallate and conjugated quercetin content (Figure 8A). *CM-1* expression was significantly positively correlated with (iso)corilagin, quinate and conjugated ellagate content (Figure 8A). *CM-2* expression was significantly positively correlated with conjugated gallate content but significantly negatively correlated with shikimate and (iso)corilagin content (Figure 8A).

The correlation analysis between genes showed that *DAHPS-2* expression was significantly positively correlated with *DAHPS-3*, *DHD/SDH-2* and *DHD/SDH-3* expression (Figure 8B). *DAHPS-3* expression was significantly positively correlated with *DHD/SDH-2* and *DHD/SDH-3* expression (Figure 8B). The *DHQS* expression was significantly positively correlated with *DHD/SDH-4*, *CS* and *CM-1* expression but significantly negatively correlated with *DHD/SDH-5* and *CM-2* expression (Figure 8B). *DHD/SDH-2* expression was significantly positively correlated with *DHD/SDH-3* and *CM-2* expression (Figure 8B). *DHD/SDH-3* expression was significantly positively correlated with *CM-2* expression (Figure 8B). *DHD/SDH-4* expression was significantly negatively correlated with *DHD/SDH-5* and *CM-2* expression (Figure 8B). *DHD/SDH-5* expression was significantly positively correlated with *CM-2* expression (Figure 8B). *CS* expression was significantly positively correlated with *CM-1* expression (Figure 8B).



(**A**)



(**B**)

Figure 8. Correlation analysis heat map: * denotes significant differences at 0.05. (**A**) Correlation analysis between shikimate-metabolism-related genes and components and (**B**) correlation analysis of shikimate-metabolism-related genes.

4. Discussion

Quinate was more abundant at all measured time points than shikimate, whose content was less than 0.2% of quinate content. Fresh apples contained a low level of shikimate, which was only used as an active intermediate metabolite [35]. The high level of quinate that accumulated in fruits of the three Chinese olive cultivars might contribute to their tart and astringent flavor. The high level of quinate in young apples could directly contribute to the bitter taste of the fruits [35]. Quinate contributed to the sour taste of kiwifruit [36]. Quinic acid is a feeding deterrent because of its astringent properties [10]. In addition, quinate has been considered as a specialized reserve compound for the biosynthesis of phenolic compounds [37]. It was assumed that after the carbon flux entered the shikimate pathway in the Chinese olive fruit, one part flowed to gallate and ellagate biosynthesis, and another part generated a large amount of quinate as a reserve for the synthesis of downstream polyphenols. Meanwhile, the remaining carbon flux was converted to shikimate without accumulation and continued to the downstream aromatic amino acid synthesis pathway.

In our study, free gallate, quercetin, luteolin and kaempferol were not detected in the three Chinese olive fruits through UPLC-MS. This might be due to the presence of gallate in the form of hydrolyzed tannins in plants [38], and flavonoids such as quercetin, kaempferol and luteolin mostly combined with sugar to form various flavonoid glycosides. In addition, the differences in cultivars and the methods of extraction and determination might also be reasons why these free-state components were not detected. Gallate biosynthesed in fruits mainly served as the phenolic moiety of HTS [1], involving gallotannins and ellagitannins. The total phenol content was 0.95% to 1.40% among the three Chinese olive fruits on the 150th DAF [29]. The conjugated ellagate content accounted for 27.43% to 40.09% of the total phenol content among the three Chinese olive fruits on the 150th DAF. High contents of conjugated gallate and ellagate were detected throughout the development and maturation of Chinese olive, implying that the biosynthesis of gallate was active in the fruit. There were differences in the contents of phenolic substances among the three cultivars. TX synthesized more ellagate, (iso)corilagin, conjugated quercetin and conjugated kaempferol; CY synthesized more conjugated luteolin; and LF synthesized a little ellagate, conjugated gallate, hyperin, conjugated quercetin, conjugated kaempferol and conjugated luteolin. This may be related to the flavor differences in the three cultivars [29].

As the entrance enzyme of the shikimate pathway, DAHPS potentially regulates the carbon flux through the shikimate pathway, which affects the synthesis of aromatic amino acids and regulates the synthesis of downstream polyphenol [25]. Inhibition of *DAHPS* expression in potato leads to slow growth and development and reduces the synthesis of secondary metabolites [25]. The *DAHPS* expression in persimmondecreased with fruit maturing, which coincided with the trend of its hydrolyzed tannin content [28]. The expression of *DAHPS* in Cumin (*Cuminum cyminum* L.) increased with UV-B stress, and the total amount of terpenoids, phenols, flavonoids and other secondary metabolites also increased significantly [39]. In our study, *DAHPS-1* expression was closely related to the accumulation of flavonoids such as hyperoside, conjugated quercetion and kaempferol among the three Chinese olive fruits. *DAHPS-1* was highly expressed in TX, and its flavonoid content was high. *DAHPS-1* in LF hardly expressed during fruit development, and its flavonoid content was very low. *DAHPS-1* might be a key gene affecting polyphenol metabolism in Chinese olive fruits.

After preliminary sequence comparison and evolutionary tree analysis, DHD/SDHs in Chinese olive could be classified into three types: the QDH type associated with quinate synthesis, the SDH type associated with gallate synthesis and the "typical" DHD/SDH type [40]. *DHD/SDH-1* and *DHD/SDH-5* belonged to the QDH type. The relatively high expression levels of *DHD/SDH-1* and *DHD/SDH-5* in *DHD/SDHs* might be one of the reasons why the quinate content was more abundant in all stages than shikimate in fruits. However, *DHD/SDH-5* expression was significantly negatively correlated with quinate content, which might play a negative regulatory role in quinate biosynthesis. The quinate content was at least partly controlled by the activities of QDH in kiwifruit [41]. *DHD/SDH-*

2 and *DHD/SDH-3* in Chinese olive fruit belonged to the type of SDH which related to gallate synthesis, and they both kept a low level after the 50th DAF in the Chinese olive fruit. *Vitis vinifera shikimate dehydrogenase gene 3* (*VvSDH3*) and *Vitis vinifera shikimate dehydrogenase gene 4* (*VvSDH4*) encoded enzymes were able to produce gallate in vitro, and they expressed at a low level after the 35th DAF in grapevine [16]. It was further confirmed that these two genes were related to gallate synthesis in the Chinese olive fruit. *DHD/SDH-4* was the "typical" type of *DHD/SDH*. *DHD/SDH-4*, *DHQS*, *CS* and *CM-1* expression and shikimate content increased with the maturing of fruit, which was sufficient to explain that shikimate metabolism was constantly strengthened to ensure the accumulation of downstream phenolic substances during the development in Chinese olive fruit. The synthesis and accumulation of quinate- and gallate-based substances showed that *SDH* family genes played an important role in shikimate metabolism of Chinese olive fruit. The accumulation of these substances and the expression of *DHD/SDHs* were worth discussing. However, the current research results seemed to be unclear and need further study.

CM is a key enzyme in regulating the carbon flux of the shikimate pathway into the phenylalanine pathway. In Petunia hybrid, the suppressed expression of plastidic *Petunia hybrida chorismate mutase gene 1* (*PhCM1*) or cytosolic *PhCM2* in RNAi lines leads to the severe reduction in the phenylalanine-derived volatiles by 60~70% and 33~64%, respectively [21,42]. In the process of later development and maturation of Chinese olive fruit (150th DAF~170th DAF), the expression of *CMs* in LF was significantly lower than that in TX and CY, coinciding with the low accumulation of total phenolics, lignins and quercetin- and kaempferol-derived flavonoids [29]. These results suggested that the *CMs* in the fruit were crucially involved in regulating phenylpropanoid metabolism of Chinese olive.

In addition, the results of the fusion expression with GFP demonstrated that the CM-1 and CM-2 of Chinese olive were localized as expected into the chloroplast/plastid and cytosol, respectively [40]. The cytosolic *Vitis vinifera chorismate mutase gene1* (*VvCM1*) was positively correlated with polyphenols and flavonoids. The enzyme encoded by this gene was not regulated by metabolites (Phe, Tyr and Trp), while plastidial *Vitis vinifera* chorismate mutase2 (VvCM2) could be activated by Trp [43]. Cytosolic AtCM2 provided the essential substrate Phe for Arabidopsis under stress conditions [20]. The expression of cytosolic *CM-2* was predominant, bearing 50~ 500-fold of the plastidial *CM-1* throughout the whole stage of fruit development and maturation, while the *CM-1* was up-regulated and the predominated *CM-2* was down-regulated, suggesting that they may play different roles in regulating the biosynthesis of aromatic amino acid and secondary phenylpropanoid metabolism of Chinese olive.

5. Conclusions

In the present study, the results revealed that quinate and gallate were synthesized and accumulated actively in Chinese olive fruit; the significantly different accumulations in phenolic compounds were demonstrated among the different cultivars. High contents of gallate, conjugated quercetin and kaempferol were detected in TX fruit, while in LF, the levels were low. Based on the results of quantitative gene expression and correlation analysis, the shikimate metabolism in Chinese olive fruit was considered to be continuously enhanced, and the expression levels of *DAHPS-1* and *CMs* were positively related to the phenolic content in fruits; they were proposed as prominent candidates for the differences in phenolic accumulation in different cultivars. The results from our study offered the foundation and framework for future understanding of the role of the shikimate pathway in phenolic metabolism in the Chinese olive fruit. In the next study, the regulatory mechanism of *SDH* family genes and *CMs* in the shikimate pathway will continue to be investigated.

Supplementary Materials: The following supporting information can be downloaded at: https://www.mdpi.com/article/10.3390/agronomy13030895/s1, Table S1: Shikimate-metabolism-related gene ORF sequences in Chinese olives.

Author Contributions: Conceptualization, J.C. and Z.G.; methodology, Z.G.; software, N.W.; validation, J.C., J.Z., Y.Z. and R.X.; investigation, F.F.; resources, T.P. and Y.Y.; data curation, J.C. and J.Z.; writing—original draft preparation, J.C. and N.W.; writing—review and editing, Z.G.; visualization, J.Z.; supervision, Z.G. and W.S.; project administration, W.S.; funding acquisition, W.S. All authors have read and agreed to the published version of the manuscript.

Funding: This research was funded by "Fujian Pilot Science and Technology Program", grant number KJy22015XA, and the "Forestry Science and Technology Extension Demonstration Project of the Central Finance", grant number 363, 2021–2023.

Data Availability Statement: Not applicable.

Conflicts of Interest: The authors declare no conflict of interest.

Appendix A

Table A1. Quantitative parameters of shikimate, quinate and phenolic compounds' determination in Chinese olive fruit by mass spectrometry MRM.

Chemical Compound	Retention Time (min)	Ionization Mode	Mass Number	Parent Ion
Shikimate	1.16	ESI(-)	174	173
Quinate	1.09	ESI(-)	192	191
Gallate	1.98	ESI(-)	170	169
Ellagate	8.16	ESI(-)	302	301
(iso)Corilagin	5.93	ESI(-)	634	633
Hyperoside	7.80	ESI(-)	464	463
Quercetin	9.45	ESI(-)	302	301
Keampferol	10.20	ESI(-)	286	285
Luteolin	9.72	ESI(-)	286	285

Table A2. Primer sequences for RT-qPCR.

Primers		Primer Sequence(5′-3′)
Actin7	F	GCATCAGTGAGATCACGTCCG
	R	CTGTGCCAATTTACGAGGGG
DAHPS-1	F	TGTCTCAACCTCCGCTCTTT
	R	CGCTGAGATGGGTTTGAGTG
DAHPS-2	F	ATAACGCACGCTAGAATG
	R	GATGTGATCGGCTGCAAAGT
DAHPS-3	F	AAATCCCCGCAGTTCTCCGC
	R	TACTGGCATTCTGGGTCTTGGT
DHQS	F	CAAGCTGTTGGTGAGACGAG
	R	ATCCAGGTAAATCGGCCCAA
DHD/SDH-1	F	GCATTGATTCCCTCACAACATTC
	R	TCTAAGTCGAGAGCCCGTCTCA
DHD/SDH-2	F	TCTCTGCACTTCCACTCACCAT
	R	ACTGGTGCGCAAATCATTGT
DHD/SDH-3	F	TTGGCAGCAGCCTATCCTCCAA
	R	CCTTTGCTTTTCGCATCTCG
DHD/SDH-4	F	CCCCTTTGCCCACTTTGTTC
	R	GCTCCCAAGTCCATGGCTAA
DHD/SDH-5	F	TGATCAGCAAAAACGGATGG
	R	CGGTCAACAAGATGGCTGAG
CS	F	TTGGGTTCTCTTCTGCCGTC
	R	CCAAATGTGGTAACACGGAAGT
CM-1	F	AAGTTGCTCCGACTCAGACCC
	R	ACCTGAACATAGAATCGTGGGAG
CM-2	F	TGAGGCTGTAGAAGAGATGGTGAA
	R	GAGGTTTCAATCTAAGCGGCG

References

1. Ye, Q.; Zhang, S.; Qiu, N.; Liu, L.; Wang, W.; Xie, Q.; Chang, Q.; Chen, Q. Identification and Characterization of Glucosyltransferase That Forms 1-Galloyl-β-d-Glucogallin in *Canarium album* L., a Functional Fruit Rich in Hydrolysable Tannins. *Molecules* **2021**, *26*, 4650. [CrossRef] [PubMed]
2. Lai, R.; Shen, C.; Feng, X.; Gao, M.; Zhang, Y.; Wei, X.; Chen, Y.; Cheng, C.; Wu, R. Integrated Metabolomic and Transcriptomic Analysis Reveals Differential Flavonoid Accumulation and Its Underlying Mechanism in Fruits of Distinct *Canarium album* Cultivars. *Foods* **2022**, *11*, 2527. [CrossRef] [PubMed]
3. Lai, R.-L.; Feng, X.; Chen, J.; Chen, Y.-T.; Wu, R.-J. The complete chloroplast genome characterization and phylogenetic analysis of *Canarium album*. *Mitochondrial DNA Part B* **2019**, *4*, 2948–2949. [CrossRef]
4. He, Z.; Xia, W. Analysis of phenolic compounds in Chinese olive (*Canarium album* L.) fruit by RPHPLC–DAD–ESI–MS. *Food Chem.* **2007**, *105*, 1307–1311. [CrossRef]
5. Yokoyama, R.; de Oliveira, M.V.V.; Kleven, B.; Maeda, H.A. The entry reaction of the plant shikimate pathway is subjected to highly complex metabolite-mediated regulation. *Plant Cell* **2021**, *33*, 671–696. [CrossRef]
6. Kanaris, M.; Poulin, J.; Shahinas, D.; Johnson, D.; Crowley, V.M.; Fucile, G.; Provart, N.; Christendat, D. Elevated tyrosine results in the cytosolic retention of 3-deoxy-d-arabino-heptulosonate 7-phosphate synthase in *Arabidopsis thaliana*. *Plant J. Cell Mol. Biol.* **2022**, *109*, 789–803. [CrossRef] [PubMed]
7. Yuan, J.; Zhong, S.; Long, Y.; Guo, J.; Yu, Y.; Liu, J. Shikimate Kinase Plays Important Roles in Anthocyanin Synthesis in Petunia. *Int. J. Mol. Sci.* **2022**, *23*, 15964. [CrossRef]
8. Habashi, R.; Hacham, Y.; Dhakarey, R.; Matityahu, I.; Holland, D.; Tian, L.; Amir, R. Elucidating the role of shikimate dehydrogenase in controlling the production of anthocyanins and hydrolysable tannins in the outer peels of pomegranate. *BMC Plant Biol.* **2019**, *19*, 476. [CrossRef]
9. Tahara, K.; Nishiguchi, M.; Funke, E.; Miyazawa, S.I.; Miyama, T.; Milkowski, C. Dehydroquinate dehydratase/shikimate dehydrogenases involved in gallate biosynthesis of the aluminum-tolerant tree species *Eucalyptus camaldulensis*. *Planta* **2020**, *253*, 3. [CrossRef]
10. Guo, J.; Carrington, Y.; Alber, A.; Ehlting, J. Molecular Characterization of Quinate and Shikimate Metabolism in *Populus trichocarpa**. *J. Biol. Chem.* **2014**, *289*, 23846–23858. [CrossRef]
11. Aydin, A.; Kurt, F.; Hürkan, K. Key aromatic amino acid players in soybean (*Glycine max*) genome under drought and salt stresses. *Biocatal. Agric. Biotechnol.* **2021**, *35*, 102094. [CrossRef]
12. Filiz, E.; Cetin, D.; Akbudak, M.A. Aromatic amino acids biosynthesis genes identification and expression analysis under salt and drought stresses in *Solanum lycopersicum* L. *Sci. Hortic.* **2019**, *250*, 127–137. [CrossRef]
13. Dyer, W.E.; Weaver, L.M.; Zhao, J.M.; Kuhn, D.N.; Weller, S.C.; Herrmann, K.M. A cDNA encoding 3-deoxy-D-arabino-heptulosonate 7-phosphate synthase from *Solanum tuberosum* L. *J. Biol. Chem.* **1990**, *265*, 1608–1614. [CrossRef]
14. Zhang, Z.-Z.; Li, X.-X.; Chu, Y.-N.; Zhang, M.-X.; Wen, Y.-Q.; Duan, C.-Q.; Pan, Q.-H. Three types of ultraviolet irradiation differentially promote expression of shikimate pathway genes and production of anthocyanins in grape berries. *Plant Physiol. Biochem.* **2012**, *57*, 74–83. [CrossRef] [PubMed]
15. Yokoyama, R.; Kleven, B.; Gupta, A.; Wang, Y.; Maeda, H.A. 3-Deoxy-D-arabino-heptulosonate 7-phosphate synthase as the gatekeeper of plant aromatic natural product biosynthesis. *Curr. Opin. Plant Biol.* **2022**, *67*, 102219. [CrossRef] [PubMed]
16. Bontpart, T.; Marlin, T.; Vialet, S.; Guiraud, J.L.; Pinasseau, L.; Meudec, E.; Sommerer, N.; Cheynier, V.; Terrier, N. Two shikimate dehydrogenases, *VvSDH3* and *VvSDH4*, are involved in gallic acid biosynthesis in grapevine. *J. Exp. Bot.* **2016**, *67*, 3537–3550. [CrossRef]
17. Huang, K.; Li, M.; Liu, Y.; Zhu, M.; Zhao, G.; Zhou, Y.; Zhang, L.; Wu, Y.; Dai, X.; Xia, T.; et al. Functional Analysis of 3-Dehydroquinate Dehydratase/Shikimate Dehydrogenases Involved in Shikimate Pathway in *Camellia sinensis*. *Front. Plant Sci.* **2019**, *10*, 1268. [CrossRef]
18. Michel, G.; Roszak, A.W.; Sauvé, V.; Maclean, J.; Matte, A.; Coggins, J.R.; Cygler, M.; Lapthorn, A.J. Structures of Shikimate Dehydrogenase AroE and Its Paralog YdiB: A common structural framework for different activities*. *J. Biol. Chem.* **2003**, *278*, 19463–19472. [CrossRef]
19. Peek, J.; Lee, J.; Hu, S.; Senisterra, G.; Christendat, D. Structural and mechanistic analysis of a novel class of shikimate dehydrogenases: Evidence for a conserved catalytic mechanism in the shikimate dehydrogenase family. *Biochemistry* **2011**, *50*, 8616–8627. [CrossRef]
20. Lynch, J.H. Revisiting the dual pathway hypothesis of Chorismate production in plants. *Hortic. Res.* **2022**, *9*, uhac052. [CrossRef]
21. Qian, Y.; Lynch, J.H.; Guo, L.; Rhodes, D.; Morgan, J.A.; Dudareva, N. Completion of the cytosolic post-chorismate phenylalanine biosynthetic pathway in plants. *Nat. Commun.* **2019**, *10*, 15. [CrossRef] [PubMed]
22. Jia, B.; Cheng, Z.; Wang, Q.; Zhang, S.; Heng, W.; Zhu, L. Characterization of the composition and gene expression involved the shikimate pathway in the exocarp of 'Dangshansuli' pear and its russet mutant. *Hortic. Environ. Biotechnol.* **2021**, *62*, 125–134. [CrossRef]
23. Zhong, S.; Chen, Z.; Han, J.; Zhao, H.; Liu, J.; Yu, Y. Suppression of chorismate synthase, which is localized in chloroplasts and peroxisomes, results in abnormal flower development and anthocyanin reduction in petunia. *Sci. Rep.* **2020**, *10*, 10846. [CrossRef] [PubMed]

24. Wilawan, N.; Ngamwonglumlert, L.; Devahastin, S.; Chiewchan, N. Changes in enzyme activities and amino acids and their relations with phenolic compounds contents in okra treated by LED lights of different colors. *Food Bioprocess. Technol.* **2019**, *12*, 1945–1954. [CrossRef]
25. Jones, J.D.; Henstrand, J.M.; Handa, A.K.; Herrmann, K.M.; Weller, S.C. Impaired Wound Induction of 3-Deoxy-D-arabino-heptulosonate-7-phosphate (DAHP) Synthase and Altered Stem Development in Transgenic Potato Plants Expressing a DAHP Synthase Antisense Construct. *Plant Physiol.* **1995**, *108*, 1413–1421. [CrossRef] [PubMed]
26. Ding, L.; Hofius, D.; Hajirezaei, M.R.; Fernie, A.R.; Börnke, F.; Sonnewald, U. Functional analysis of the essential bifunctional tobacco enzyme 3-dehydroquinate dehydratase/shikimate dehydrogenase in transgenic tobacco plants. *J. Exp. Bot.* **2007**, *58*, 2053–2067. [CrossRef]
27. Herrmann, K.M. The shikimate pathway as an entry to aromatic secondary metabolism. *Plant Physiol.* **1995**, *107*, 7–12. [CrossRef]
28. Akagi, T.; Ikegami, A.; Suzuki, Y.; Yoshida, J.; Yamada, M.; Sato, A.; Yonemori, K. Expression balances of structural genes in shikimate and flavonoid biosynthesis cause a difference in proanthocyanidin accumulation in persimmon (*Diospyros kaki* Thunb.) fruit. *Planta* **2009**, *230*, 899–915. [CrossRef]
29. Cai, J.; Wang, J.; Zhao, J.; Pan, T.; Guo, Z.; She, W. Metabolomics and Its Difference of Chinese Olive Fruit of Different Varieties (lines) During the Ripening Period. *Chin. J. Trop. Crops* **2022**, *43*, 2304–2315. (In Chinese) [CrossRef]
30. Wang, J.; Cai, J.; Zhao, J.; Guo, Z.; Pan, T.; Yu, Y.; She, W. Enzyme Activities in the Lignin Metabolism of Chinese Olive (*Canarium album*) with Different Flesh Characteristics. *Horticulturae* **2022**, *8*, 408. [CrossRef]
31. Reichel, M.; Carle, R.; Sruamsiri, P.; Neidhart, S. Changes in flavonoids and nonphenolic pigments during on-tree maturation and postharvest pericarp browning of litchi (*Litchi chinensis* Sonn.) as shown by HPLC-MS^n. *J. Agric. Food Chem.* **2011**, *59*, 3924–3939. [CrossRef] [PubMed]
32. Muir, S.R.; Collins, G.J.; Robinson, S.; Hughes, S.; Bovy, A.; Ric De Vos, C.H.; van Tunen, A.J.; Verhoeyen, M.E. Overexpression of petunia chalcone isomerase in tomato results in fruit containing increased levels of flavonols. *Nat. Biotechnol.* **2001**, *19*, 470–474. [CrossRef] [PubMed]
33. Huang, M. Measurement of Hyperoside Content, Cloning and Expression of the Synthesis Genes in *Canarium album*. Master's Thesis, Fujian Agriculture and Forestry University, Fujian, China, 2017. (In Chinese).
34. Livak, K.J.; Schmittgen, T.D. Analysis of relative gene expression data using real-time quantitative PCR and the 2(-Delta Delta C(T)) Method. *Methods* **2001**, *25*, 402–408. [CrossRef] [PubMed]
35. Hulme, A.C. Quinic and shikimic acids in fruits. *Qual. Plant. Mater. Veg.* **1958**, *3*, 468–473. [CrossRef]
36. Marsh, K.; Rossiter, K.; Lau, K.; Walker, S.; Gunson, A.; Macrae, E. The use of fruit pulps to explore flavour in kiwifruit. *Acta Hortic.* **2003**, *610*, 229–237. [CrossRef]
37. Ossipov, V.; Chernov, A.V.; Zrazhevskaya, G.; Shein, I.V. Quinate:NAP(P)$^+$-oxidoreductase from Larix sibirica: Purification, characterization and function. *Trees* **1995**, *10*, 46–51. [CrossRef]
38. Guo, L.; Qiang, T.; Ma, Y.; Ren, L.; Dai, T. Purification and characterization of hydrolysable tannins extracted from *Coriaria nepalensis* bark using macroporous resin and their application in gallic acid production. *Ind. Crops Prod.* **2021**, *162*, 113302. [CrossRef]
39. Ghasemi, S.; Kumleh, H.H.; Kordrostami, M. Changes in the expression of some genes involved in the biosynthesis of secondary metabolites in *Cuminum cyminum* L. under UV stress. *Protoplasma* **2019**, *256*, 279–290. [CrossRef]
40. Cai, J. Cloning and Expression Analysis of Shikimic Acid Metabolism Related Genes During the Development of Chinese Olive Fruit. Master's Thesis, Fujian Agriculture and Forestry University, Fujian, China, 2022. (In Chinese).
41. Marsh, K.B.; Boldingh, H.L.; Shilton, R.S.; Laing, W.A. Changes in quinic acid metabolism during fruit development in three kiwifruit species. *Funct. Plant Biol. FPB* **2009**, *36*, 463–470. [CrossRef]
42. Colquhoun, T.; Schimmel, B.; Kim, J.Y.; Reinhardt, D.; Cline, K.; Clark, D. A petunia chorismate mutase specialized for the production of floral volatiles. *Plant J. Cell Mol. Biol.* **2009**, *61*, 145–155. [CrossRef]
43. Li, X. Collaborative Expression Mechanism between Shikimate Pathway and Flavonoid Metabolism. Ph.D. Thesis, China Agricultural University, Beijing, China, 2016. (In Chinese).

Disclaimer/Publisher's Note: The statements, opinions and data contained in all publications are solely those of the individual author(s) and contributor(s) and not of MDPI and/or the editor(s). MDPI and/or the editor(s) disclaim responsibility for any injury to people or property resulting from any ideas, methods, instructions or products referred to in the content.